Physics of Fluids ARTICLE pubs.aip.org/aip/pof

# Hydrodynamic theory of premixed flames under Darcy's law

Cite as: Phys. Fluids **36**, 123620 (2024); doi: 10.1063/5.0248749
Submitted: 13 November 2024 · Accepted: 28 November 2024 ·
Published Online: 12 December 2024



Prabakaran Rajamanickam[a] and Joel Daou[b]

## AFFILIATIONS

Department of Manchester, University of Manchester, Manchester M13 9PL, United Kingdom

[a]**Present address:** Department of Mathematics & Statistics, University of Strathclyde, Glasgow G1 1XQ, United Kingdom
[b]**Author to whom correspondence should be addressed:** joel.daou@manchester.ac.uk

## ABSTRACT

This paper investigates the theoretical implications of applying Darcy's law to premixed flames, a topic of growing interest in research on flame propagation in porous media and confined geometries. A multiple-scale analysis is carried out treating the flame as a hydrodynamic discontinuity in density, viscosity, and permeability. The analysis accounts in particular for the inner structure of the flame. A simple model is derived allowing the original conservation equations to be replaced by Laplace's equation for pressure, applicable on both sides of the flame front, subject to specific conditions across the front. Such model is useful for investigating general problems under confinement including flame instabilities in porous media or Hele-Shaw channels. In this context, two Markstein numbers are identified, for which explicit expressions are provided. In particular, our analysis reveals novel contributions to the local propagation speed arising from discontinuities in the tangential components of velocity and gravitational force, which are permissible in Darcy's flows to leading order, but not in flows obeying Euler or Navier–Stokes equations.





## I. INTRODUCTION

The study of flame propagation in porous media and narrow confined geometries, such as Hele-Shaw cells, is an active research area.[1–5] One key distinction between normal flames and flames in strongly confined media lies in their hydrodynamic behavior. In porous media, fluid dynamics is primarily governed by Darcy's law and so is the case in slender Hele-Shaw cells. Several recent numerical investigations have successfully employed Darcy's law to characterize flame propagation in Hele-Shaw cells, under the assumption of near-adiabatic walls.[3,6–8]

A fundamental question remains however: What are the theoretical implications of applying Darcy's law to premixed flames? A recent study by Daou and Rajamanickam[9] addressed this question by treating the flame as a hydrodynamic discontinuity and investigating its instabilities. The study builds upon earlier research by Joulin and Sivashinsky[10] and Miroshnichenko *et al.*,[11] which utilized the so-called Euler–Darcy model. Despite these advancements, a comprehensive theoretical description of premixed flames under Darcy's law, accounting for their internal structure, remains an open problem. This paper is dedicated to addressing this challenging problem.

The classical hydrodynamic theory of premixed flames, based on the Navier–Stokes equations, was developed in pioneering contributions by Sivashinsky,[12] Clavin and Williams,[13] Pelce and Clavin,[14] Matalon and Matkowsky,[15] and Clavin and Joulin.[16] Notably, the latter two studies presented comprehensive theories that accounted for finite-amplitude flame wrinkling. Subsequent research has extended this theory to various contexts.[16–24]

In this paper, we embark on a theoretical analysis of premixed flames assumed to be governed by Darcy's law, an assumption which is motivated by asymptotic analyses in the narrow channel limit.[3,7,9] One of our main aims is to understand the hydrodynamic aspects of confinement on flame propagation, which are poorly understood. To isolate and highlight these aspects, intimately related to Darcy's law, we consider a simplified configuration involving an equidiffusive reacting mixture (unity Lewis number) and neglect heat-loss effects. As we shall see, our study will result in the derivation of a simplified hydrodynamic model for flame propagation, involving specific jump conditions across the flame front and explicit formulas for the so-called Markstein numbers, characterizing the local propagation speed. The study will also reveal novel contributions to the local propagation speed arising from leading-order tangential discontinuities in the velocity and the gravitational force, which are not present in conventional flame theory.

## II. PROBLEM FORMULATION

Consider a premixed flame propagating through an unburnt gas mixture containing a deficient reactant. This mixture possesses constant values of density $\rho_u$, viscosity $\mu_u$, permeability $\kappa_u$, and thermal diffusivity $D_u$. Similarly, the burnt gas mixture behind the flame is characterized by constant properties, $\rho_b$, $\mu_b$, $\kappa_b$, and $D_b$. For Hele-Shaw channels, $\kappa_u = \kappa_b = h^2/12$, where $h$ is the channel width. We assume that the characteristic length scale, $L$, of flame wrinkling is significantly larger than the flame thickness $\delta_L = D_u/S_L$, where $S_L$ represents the planar, laminar flame speed with respect to the unburnt gas. Our theoretical framework is based on a small expansion parameter, $\varepsilon$, defined as

$$\varepsilon = \frac{\delta_L}{L} \ll 1. \tag{1}$$

For convenience, we non-dimensionalize physical quantities using $L$ as the length scale, $L/S_L$ as the time scale, $S_L$ as the velocity scale, and $\mu_u D_u/\varepsilon\kappa_u$ as the pressure scale. As previously mentioned, the Lewis number of the reacting mixture will be assumed equal to one, and heat-loss effects will be ignored. Under these conditions, the mass fraction $Y$ of the reactant is related to the temperature $T$ by $Y/Y_u = 1 - (T/T_u - 1)/q$, where $q$ defines the flame temperature by the relation $T_b = T_u(1+q)$. All physical properties of the fluid are non-dimensionalized using their respective values on the unburnt gas mixture, and the non-dimensional temperature $\theta$ is defined by $\theta = (T - T_u)/qT_u$ such that it approaches zero in the unburnt gas and unity in the burnt gas. A schematic illustration of the premixed flame, in non-dimensional units, is depicted in Fig. 1.

Let us introduce the familiar $G$-equation[25]

$$\rho\left(\frac{\partial G}{\partial t} + \mathbf{v}\cdot\nabla G\right) = \dot{m}|\nabla G|, \tag{2}$$

which involves $\dot{m}(\mathbf{x}, t)$, the normal mass flux crossing a given level set $G(\mathbf{x}, t) = \text{const}$. The function $G(\mathbf{x}, t)$ defines for a given level set the local normal unit vector $\mathbf{n} = \nabla G/|\nabla G|$ pointing toward the burnt gas. We identify the level $G = 0$ to be the flame-front location from the viewpoint of the outer hydrodynamic zone. Furthermore, the reaction-sheet location will be identified with the level $G = \varepsilon a$, where $a$ is some constant.

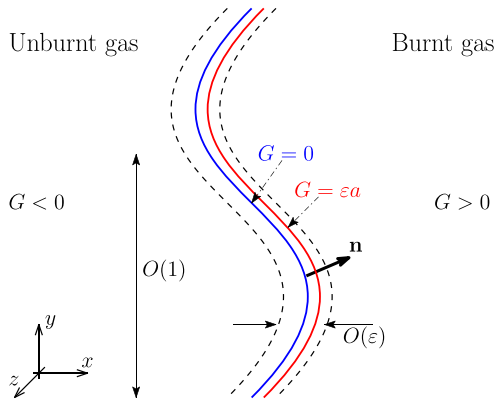


**FIG. 1.** Schematic illustration of a curved premixed flame propagating into a fresh mixture. The location of the flame front corresponds to a level set $G = 0$ of the field $G(\mathbf{x}, t)$; the location of the reaction sheet corresponds to the level set $G = \varepsilon a$.

On each side of the reaction sheet $G \neq \varepsilon a$, the following governing equations are assumed to hold:

$$\frac{\partial \rho}{\partial t} + \nabla\cdot(\rho\mathbf{v}) = 0, \tag{3}$$

$$-\mu\mathbf{v} = \nabla p - \rho\mathbf{g}, \tag{4}$$

$$\rho\frac{\partial\theta}{\partial t} + \rho\mathbf{v}\cdot\nabla\theta = \varepsilon\nabla\cdot(\lambda\nabla\theta), \tag{5}$$

$$\rho = \rho(\theta), \quad \mu = \mu(\theta), \quad \lambda = \lambda(\theta), \tag{6}$$

where $\mathbf{g}$ is the non-dimensional gravity vector, whose magnitude, $|\mathbf{g}| = \rho_u g\kappa_u/\mu_u S_L$, measures the strength of the gravitational force. The function $\mu = \mu(\theta)$ is assumed to incorporate both fluid viscosity and permeability.

Across the reaction sheet (not the flame front), all physical variables satisfy certain jump conditions, which are well established and are expressed readily in terms of a small-scale flame coordinate $\zeta$, which is defined by

$$\zeta = \frac{1}{\varepsilon}(G - \varepsilon a). \tag{7}$$

At the reaction sheet, $\zeta = 0$, we have

$$[[\mathbf{v}]] = [[p]] = [[\theta]] = \lambda|\nabla G|\left[\left[\frac{\partial\theta}{\partial\zeta}\right]\right] + 1 = 0, \tag{8}$$

where $[[\varphi]] \equiv \varphi|_{\zeta=0^+} - \varphi|_{\zeta=0^-}$. In summary, $G = 0$ (or $\zeta = -a$) corresponds to the flame front, i.e., the front location seen from the viewpoint of the outer hydrodynamic zone and $G = \varepsilon a$ (or $\zeta = 0$) corresponds to the reaction sheet. Traditionally, one usually sets $a = 0$, although it is important to recognize that the end results of the analysis will depend on $a$ as can be inferred from the analysis by Bechtold and Matalon[26] and as such we will not discard the constant parameter $a$.

## III. MULTIPLE-SCALE ANALYSIS

The asymptotic solution to the problem described above in the limit $\varepsilon \to 0$ is carried out now using multiple-scale analysis, following closely Keller and Peters.[20,27] In our multiple-scale analysis, all physical variables, except $G$ (and therefore $\mathbf{n}$), are assumed to depend on both the large-scale hydrodynamic coordinates $(\mathbf{x}, t)$ and the small-scale flame coordinate, $\zeta$. Any physical variable $\varphi$ is expanded in a power series in $\varepsilon$

$$\varphi = \varphi_0(\zeta, \mathbf{x}, t) + \varepsilon\varphi_1(\zeta, \mathbf{x}, t) + \cdots. \tag{9}$$

It is important to note that $G$ cannot be a function of $\zeta$, as $G$ itself defines $\zeta$ (7). Moreover, we shall assume from the outset that the function $G(\mathbf{x}, t)$ is described with arbitrary accuracy in powers of $\varepsilon$, and as a result, we do not expand the function $G$, following Clavin and Graña-Otero[23] and Clavin and Searby.[28] This assumption does affect the intermediate steps of the analysis, but not the final uniformly valid solution.

For physical variables depending also on the coordinate $\zeta$, the transformation rules for derivatives with respect to large-scale coordinates $(x^i, t)$ are given by

$$\frac{\partial}{\partial x^i} \mapsto \frac{1}{\varepsilon}\frac{\partial G}{\partial x^i}\frac{\partial}{\partial\zeta} + \frac{\partial}{\partial x^i}, \quad \frac{\partial}{\partial t} \mapsto \frac{1}{\varepsilon}\frac{\partial G}{\partial t}\frac{\partial}{\partial\zeta} + \frac{\partial}{\partial t}. \tag{10}$$

Any function, which is independent of $\zeta$, can be regarded as variables corresponding to outer hydrodynamic zone. Furthermore, the continuity equation can be rewritten, when combined with the $G$-equation, as

$$\frac{\partial \rho}{\partial t} + \nabla \cdot (\rho \mathbf{v}) = -\frac{|\nabla G|}{\varepsilon} \frac{\partial \dot{m}}{\partial \zeta}. \tag{11}$$

This has a simple interpretation: the continuity equation based on the outer coordinates $(\mathbf{x}, t)$ has a non-zero source term whenever the normal mass flux $\dot{m}$ varies with the inner coordinate $\zeta$.

### A. Structure of the locally planar flame

At the leading order, we obtain

$$\frac{\partial \dot{m}_0}{\partial \zeta} = \frac{\partial p_0}{\partial \zeta} = 0, \quad \frac{\dot{m}_0}{|\nabla G|} \frac{\partial \theta_0}{\partial \zeta} = \frac{\partial}{\partial \zeta} \left( \lambda_0 \frac{\partial \theta_0}{\partial \zeta} \right). \tag{12}$$

The solution, subject to the jump conditions (8), is given by

$$p_0 = P_0(\mathbf{x}, , t), \quad \dot{m}_0 = \dot{M}_0(\mathbf{x}, t) = 1, \quad \theta_0 = \begin{cases} e^{\hat{\zeta}/|\nabla G|}, & \zeta < 0, \\ 1, & \zeta > 0, \end{cases} \tag{13}$$

where $\hat{\zeta} = \int_0^\zeta d\zeta/\lambda_0$. The outer functions $\dot{M}_0(\mathbf{x}, t)$ and $P_0(\mathbf{x}, t)$ are continuous across $G = 0$. The continuity of $P_0(\mathbf{x}, t)$, which is specific to Darcy's law, will be shown later.

### B. Leading-order flow field

At the first order, the momentum equation yields

$$-\mu_0 \mathbf{v}_0 = \nabla P_0 - \rho_0 \mathbf{g} + \nabla G \frac{\partial p_1}{\partial \zeta}. \tag{14}$$

The pressure gradient $\partial p_1/\partial \zeta$ can be eliminated by multiplying the equation vectorially with $\mathbf{n}$ to result in $-\mu_0 \mathbf{v}_0 \times \mathbf{n} = \nabla P_0 \times \mathbf{n} - \rho_0 \mathbf{g} \times \mathbf{n}$. Another cross product with $\mathbf{n}$ from the left yields the tangential component of $\mathbf{v}_0$, i.e., $\mathcal{P}\mathbf{v}_0 = \mathbf{n} \times (\mathbf{v}_0 \times \mathbf{n})$, where $\mathcal{P} = \mathbf{I} - \mathbf{nn}$ is the projection (matrix) operation of a vector onto the tangent surface. On the other hand, the normal component $\mathbf{v}_0 \cdot \mathbf{n}$ can be determined from the leading-order $G$-equation $\rho_0(\partial G/\partial t + \mathbf{v}_0 \cdot \nabla G) = |\nabla G|$. Combining the two components, we obtain

$$\mathbf{v}_0 = \left( \frac{1}{\rho_0} - \frac{1}{|\nabla G|} \frac{\partial G}{\partial t} \right) \mathbf{n} - \frac{\mathcal{P}}{\mu_0} (\nabla P_0 - \rho_0 \mathbf{g}). \tag{15}$$

It is convenient to introduce an auxiliary outer function $\mathbf{V}_0(\mathbf{x}, t)$ defined for $G \neq 0$ by

$$\nabla \cdot \mathbf{V}_0 = 0, \quad -\bar{\mu}\, \mathbf{V}_0 = \nabla P_0 - \bar{\rho} \mathbf{g}, \tag{16}$$

$$\bar{\rho} \frac{\tilde{D} G}{\tilde{D} t} \equiv \bar{\rho} \left( \frac{\partial G}{\partial t} + \mathbf{V}_0 \cdot \nabla G \right) = |\nabla G|, \tag{17}$$

and involving the (outer) constants $\bar{\rho}$ and $\bar{\mu}$ given by

$$\bar{\rho} = \begin{cases} 1, & G < 0, \\ \rho_f \equiv \rho(1), & G > 0, \end{cases} \quad \bar{\mu} = \begin{cases} 1, & G < 0, \\ \mu_f \equiv \mu(1), & G > 0. \end{cases} \tag{18}$$

From the last two equations in (16) and (17), it follows as in the derivation of (15) that

$$\mathbf{V}_0 = \left( \frac{1}{\bar{\rho}} - \frac{1}{|\nabla G|} \frac{\partial G}{\partial t} \right) \mathbf{n} - \frac{\mathcal{P}}{\bar{\mu}} (\nabla P_0 - \bar{\rho} \mathbf{g}), \tag{19}$$

and therefore, on combining (15) and (19), that

$$\mathbf{v}_0 - \mathbf{V}_0 = \frac{\bar{\rho} - \rho_0}{\bar{\rho} \rho_0} \mathbf{n} - \mathcal{P} \left( \frac{\mu_0 - \bar{\mu}}{\mu_0} \mathbf{V}_0 + \frac{\bar{\rho} - \rho_0}{\mu_0} \mathbf{g} \right). \tag{20}$$

This equation implies that $\mathbf{v}_0 - \mathbf{V}_0$ vanishes exponentially as $\zeta \to -\infty$ and is identically zero for $\zeta > 0$. Thus, the flow field $(\mathbf{V}_0, P_0)$, which is incompressible and obeys Darcy's law for $G \neq 0$ according to (16) and (17), is indeed the outer flow to leading order.

### C. First correction to normal mass flux

The continuity equation (11) at the first order implies

$$|\nabla G| \frac{\partial \dot{m}_1}{\partial \zeta} = -\frac{\partial \rho_0}{\partial t} - \nabla \cdot (\rho_0 \mathbf{v}_0), \tag{21}$$

$$= \frac{\tilde{D}}{\tilde{D} t} (\bar{\rho} - \rho_0) - \nabla \cdot [\rho_0 (\mathbf{v}_0 - \mathbf{V}_0)], \tag{22}$$

where the last expression follows from the previous one, upon adding and subtracting $\nabla \cdot (\rho_0 \mathbf{V}_0)$ and using the condition $\nabla \cdot \mathbf{V}_0 = 0$ and the notation of (17). We now integrate this equation from $\zeta = -\infty$ to an arbitrary location $\zeta$ in the preheat zone, noting that the integration can be commuted with the (outer) differential operators on the right side. The integration is conveniently performed by changing the integration variable to $\theta_0 = e^{\hat{\zeta}/|\nabla G|}$, as given by (13), so that $d\zeta = d\theta_0 \, |\nabla G| \lambda_0/\theta_0$. Carrying out the integration and using (20), we find

$$|\nabla G| \left[ \dot{m}_1 - \dot{M}_1(\mathbf{x}, t) \right] = \frac{\tilde{D}}{\tilde{D} t} (\hat{\mathscr{I}}_1 |\nabla G|) - \frac{1}{\bar{\rho}} \nabla \cdot (\hat{\mathscr{I}}_1 \nabla G) + \nabla \cdot \left[ |\nabla G| \mathscr{P} (\hat{\mathscr{I}}_2 \mathbf{V}_0 + \hat{\mathscr{I}}_3 \mathbf{g}) \right], \tag{23}$$

for $\zeta < 0$, where $\dot{M}_1(\mathbf{x}, t)$ is the integration constant and

$$\hat{\mathscr{I}}_1(\theta_0) = \int_0^{\theta_0} \frac{\lambda_0}{\theta_0} (\bar{\rho} - \rho_0) d\theta_0,$$

$$\hat{\mathscr{I}}_2(\theta_0) = \int_0^{\theta_0} \frac{\rho_0 \lambda_0}{\mu_0 \theta_0} (\mu_0 - \bar{\mu}) d\theta_0,$$

$$\hat{\mathscr{I}}_3(\theta_0) = \int_0^{\theta_0} \frac{\rho_0 \lambda_0}{\mu_0 \theta_0} (\bar{\rho} - \rho_0) d\theta_0.$$

The function $\dot{m}_1 - \dot{M}_1$ is seen to vanish exponentially as $\zeta \to -\infty$ (since $\theta_0 \to 0$ in the integrals) and identically for $\zeta > 0$ (since the rhs of (22) is then zero). Thus, $\dot{M}_1(\mathbf{x}, t)$ corresponds to the first-order correction to the normal mass flux $\dot{m}$ in the outer region. Evaluated at the location of the reaction sheet, $\zeta = 0$ where $\theta_0 = 1$, the integrals $(\hat{\mathscr{I}}_1, \hat{\mathscr{I}}_2, \hat{\mathscr{I}}_3)$ become $(\mathscr{I}_1, \mathscr{I}_2, \mathscr{I}_3) \equiv (\hat{\mathscr{I}}_1(1), \hat{\mathscr{I}}_2(1), \hat{\mathscr{I}}_3(1))$ and come out of the derivatives in (23). Dividing by $|\nabla G|$ and simplifying using a few vector identities,[29] we obtain for $\dot{m}_1 - \dot{M}_1$ evaluated at $\zeta = 0$ the expression

$$\dot{m}_1 - \dot{M}_1 = -\left[ \frac{\mathscr{I}_1}{\bar{\rho}} + (\mathscr{I}_2 \mathbf{V}_0 + \mathscr{I}_3 \mathbf{g}) \cdot \mathbf{n} \right] \nabla \cdot \mathbf{n} - (\mathscr{I}_1 + \mathscr{I}_2) \mathbf{nn} : \nabla \mathbf{V}_0. \tag{24}$$

We next examine the temperature equation at the first order which implies that

$$|\nabla G|^2\frac{\partial}{\partial\zeta}\left(\lambda_0\frac{\partial\theta_1}{\partial\zeta}+\lambda_1\frac{\partial\theta_0}{\partial\zeta}\right)-\dot m_0|\nabla G|\frac{\partial\theta_1}{\partial\zeta}$$
$$=|\nabla G|\frac{\partial(\dot m_1\theta_0)}{\partial\zeta}+\frac{\partial(\rho_0\theta_0)}{\partial t}+\nabla\cdot(\rho_0\mathbf{v}_0\theta_0)$$
$$-\nabla^2G\lambda_0\frac{\partial\theta_0}{\partial\zeta}-\nabla G\cdot\left[\frac{\partial}{\partial\zeta}(\lambda_0\nabla\theta_0)+\nabla\left(\lambda_0\frac{\partial\theta_0}{\partial\zeta}\right)\right]. \quad (25)$$

In the burnt gas, $\zeta>0$, the solution for $\theta_1$ is simply $\theta_1=0$. In the unburnt gas, it is sufficient to integrate Eq. (25) from $\zeta=-\infty$ to $\zeta=0^-$ to determine $\dot M_1$. The integration is subject to the requirement that $\theta_1$ and its gradient vanish as $\zeta\to-\infty$ and the conditions (8) at the reaction sheet which imply that

$$\theta_1=0\,,\quad |\nabla G|\left(\lambda_0\frac{\partial\theta_1}{\partial\zeta}+\lambda_1\frac{\partial\theta_0}{\partial\zeta}\right)=0\quad\text{at}\quad\zeta=0^-\,. \quad (26)$$

Performing the integration, we obtain after some simplifications[30] the expression

$$\dot M_1=\left[\frac{\mathscr{J}_1}{\bar\rho}+(\mathscr{J}_2\mathbf{V}_0+\mathscr{J}_3\mathbf{g})\cdot\mathbf{n}\right]\nabla\cdot\mathbf{n}+(\mathscr{J}_1+\mathscr{J}_2)\mathbf{nn}:\nabla\mathbf{V}_0, \quad (27)$$

where

$$\mathscr{J}_1=\int_0^1\frac{\lambda_0}{\theta_0}[\bar\rho-\rho_0(1-\theta_0)]d\theta_0, \quad (28)$$

$$\mathscr{J}_2=\int_0^1\frac{\rho_0\lambda_0}{\mu_0\theta_0}(\mu_0-\bar\mu)(1-\theta_0)d\theta_0, \quad (29)$$

$$\mathscr{J}_3=\int_0^1\frac{\rho_0\lambda_0}{\mu_0\theta_0}(\bar\rho-\rho_0)(1-\theta_0)d\theta_0. \quad (30)$$

It is worth pointing out at this stage that the influence of the constant parameter $a$ appearing in Eq. (7) and in Fig. 1 is buried in these integrals. This is so since $\bar\rho$ and $\bar\mu$ have jumps at $\zeta=-a$ or $G=0$, which corresponds to an isotherm contour $\theta_0=\theta_*$ where $\theta_*\equiv e^{\hat\zeta_*/|\nabla G|}$ with $\hat\zeta_*=-\int_{-a}^0 d\zeta/\lambda_0$. For illustration, the expression for $\mathscr{J}_1$ is given by

$$\mathscr{J}_1=\int_0^{\theta_*}\frac{\lambda_0}{\theta_0}[1-\rho_0(1-\theta_0)]d\theta_0+\int_{\theta_*}^1\frac{\lambda_0}{\theta_0}[\rho_f-\rho_0(1-\theta_0)]d\theta_0, \quad (31)$$

and similar expressions can be written for $\mathscr{J}_2$ and $\mathscr{J}_3$. To summarize, it is convenient to view $\theta_*$ as a prescribed parameter, determining $a$ and allowing to define the flame front as the iso-temperature surface $\theta=\theta_*$. This observation has been emphasized in the recent works by Giannakopoulos *et al.*[31,32]

### D. Continuity of the pressure field

The continuity of the pressure field follows directly from the Darcy's law $\nabla p=-\mu\mathbf{v}+\rho\mathbf{g}$. Provided the terms on the right-hand side experience at most finite jumps across the flame, as it is the case, integration of this equation across the flame front shows that $p$ is continuous across the flame. This statement holds true at all orders of $\varepsilon$.

## IV. SUMMARY OF RESULTS

At this stage, we are able to describe the flame in a Darcy's flow as a hydrodynamic interface across which specific jump conditions, correct to order $\varepsilon$, must be satisfied. To this end, let us write $\mathbf{V}=\mathbf{V}_0+\varepsilon\mathbf{V}_1$, $P=P_0+\varepsilon P_1$, $\dot M=\dot M_0+\varepsilon\dot M_1$ and drop the overbars for $\bar\rho$ and $\bar\mu$. Then, the problem is governed on each side of the flame front, $G\neq0$, by the equations

$$\nabla\cdot\mathbf{V}=0,\quad -\mu\mathbf{V}=\nabla P-\rho\mathbf{g}\quad\Rightarrow\quad\nabla^2P=0. \quad (32)$$

The corresponding jump conditions to be satisfied at the flame front, $G=0$, are

$$[[\rho(\mathbf{V}-\mathbf{U})\cdot\mathbf{n}]]=0,\quad [[P]]=0, \quad (33)$$

where $[[\varphi]]\equiv\varphi|_{G=0^+}-\varphi|_{G=0^-}$, and $\mathbf{U}\cdot\mathbf{n}=-(\partial G/\partial t)/|\nabla G|$ is the normal frame-front velocity. In addition, the problem is constrained by the kinematic condition

$$\rho\left(\frac{\partial G}{\partial t}+\mathbf{V}\cdot\nabla G\right)=\dot M|\nabla G|, \quad (34)$$

characterizing the propagation of the flame front. This condition is to be applied either at $G=0^-$ (unburnt gas side where $\rho=1$) or at $G=0^+$ (burnt gas side where $\rho=\rho_f$). It involves the normal mass flux $\dot M$ given by

$$\dot M=1+\varepsilon(\mathscr{M}_c\nabla\cdot\mathbf{n}+\mathscr{M}_s\mathbf{nn}:\nabla\mathbf{V}), \quad (35)$$

and the two Markstein numbers

$$\mathscr{M}_c=\frac{\mathscr{J}_1}{\rho}+(\mathscr{J}_2\mathbf{V}+\mathscr{J}_3\mathbf{g})\cdot\mathbf{n}\,,\quad\mathscr{M}_s=\mathscr{J}_1+\mathscr{J}_2. \quad (36)$$

The integrals $\mathscr{J}_1$, $\mathscr{J}_2$, and $\mathscr{J}_3$ appearing in the Markstein numbers depend on the choice for the flame-front location within the inner zone. As mentioned earlier, the location of the flame front can be specified by selecting an iso-temperature surface $\theta=\theta_*$ with $0<\theta^*<1$. It is worth nothing here that the selection of the optimal $\theta_*$ when comparing quantitatively with numerical or experimental data seems to be a delicate matter, as discussed by Giannakopoulos *et al.*[31] within the common framework of Navier–Stokes flows. In the present framework of Darcy's flows, similar dedicated numerical studies in prototypical configurations are needed in future investigations to assess the quantitative influence of the choice of $\theta_*$.

In summary, the original problem governed by the equations of Sec. II has been reduced to the simpler problem of solving Laplace's equation $\nabla^2P=0$ for $G\neq0$ subject to the conditions (33) and (34).

A key novel result of this study corresponds to the formulas (36) for the Markstein numbers which contain new terms that are specific to Darcy's law. These formulas should be compared with the corresponding formulas[28] based on Navier–Stokes equations which, when applied under the same assumptions used here, imply that

$$\mathscr{M}_c=\frac{\mathscr{J}_1}{\rho}\,,\quad\mathscr{M}_s=\mathscr{J}_1. \quad (37)$$

It is worth noting that the new terms in (36) can be attributed to the Darcy's law allowing the presence of discontinuities to leading order in the tangential velocity across the flame. Such discontinuities arise either due to viscosity jumps, $[[\mu]]\neq0$, or to jumps in the gravitation

term, $[[\rho g_t]] \neq 0$ where the subscript $t$ denotes tangential components. This can be seen from the jump condition $[[\mu V_t]] = [[\rho g_t]]$ which follows readily from an integration of the tangential component of Darcy's equation across the flame and use of the continuity of pressure, $[[P]] = 0$. Such discontinuities of the tangential component of velocity across the flame do not occur (at least to leading order) for flames in a flow obeying Euler or Navier–Stokes equations, see, e.g., Matalon and Matkowsky.[15] Interestingly, the curvature Markstein number $\mathscr{M}_c$ in (36) depends not only on the fluid physio-chemical properties but also on the normal components of the flow velocity and gravity.

Equations (32)–(34) are versatile, applicable to various problems of interest, involving both numerical and theoretical analysis. In particular, they include explicit expressions for the Markstein numbers, which were to date unavailable, but which are valuable when studying flame propagation and stability under confinement. Such expressions are useful, e.g., to complement our recent work[9] which explored the stability of a planar premixed flame propagating against a uniformly moving fresh mixture, accounting for the presence of gravity, represented by vector $\mathbf{g}$ pointing in the direction of flame propagation. We derived in this case a dispersion relation linking the perturbation growth rate ($s$) to the transverse wavenumber magnitude ($k$), given by

$$s = \frac{ak - bk^2}{1 + ck},$$

where

$$a = \frac{r-1}{1+m} + \frac{1-m}{1+m}\mathscr{V} - \frac{r-1}{1+m}\frac{m}{r}|\mathbf{g}|, \quad b = \frac{r+m}{1+m}\mathscr{M}_c + a\mathscr{M}_s,$$
$$c = \frac{r-1}{1+m}\mathscr{M}_s.$$

Here, $k$ and $s$ are measured in units of $\delta_L^{-1}$ and $S_L/\delta_L$, $r = 1/\rho_f$ is the unburnt-to-burnt gas density ratio, $m = 1/\mu_f$ is the viscosity ratio, and $\mathscr{V}$ is the speed of the oncoming flow of fresh mixture, measured with $S_L$. The three terms in the expression for $a$ correspond, respectively, to Darrieus–Landau, Saffman–Taylor, and Rayleigh–Taylor instabilities. The oncoming flow opposes flame propagation when $\mathscr{V} > 0$ and aids flame propagation when $\mathscr{V} < 0$. Similarly, $|\mathbf{g}| > 0$ corresponds to downward flame propagation and $|\mathbf{g}| < 0$ to upward flame propagation. More detailed analyses and implications of the dispersion relation can be found in Daou and Rajamanickam.[9]

To close this paper, we mention worthwhile extensions of this work in future investigations. The first natural extension is to account for non-unit values of the Lewis numbers, as typically encountered in applications. In principle, this is straightforward to carry out despite the lengthy algebraic manipulations involved, as classically done within the so-called near-equidiffusive approximation.[12] Another important issue to address is the influence of heat losses, which is a significant aspect to consider when describing the effect of confinement on flames. This complicating factor has been purposely sidelined in this paper in order to clarify the poorly understood hydrodynamic aspect associated with flame propagation in a Darcy's flow. The effect of including heat losses in our model is definitely worth investigating, since it is anticipated to modify the Markstein numbers, as can be inferred from similar studies.[19,20,22]

## ACKNOWLEDGMENTS

This work was supported by the UK EPSRC through Grant No. EP/V004840/1 and Grant No. APP39756. The authors are grateful to Professor Paul Clavin for insightful comments on the paper.

## AUTHOR DECLARATIONS

### Conflict of Interest

The authors have no conflicts to disclose.

### Author Contributions

**Prabakaran Rajamanickam:** Conceptualization (equal); Formal analysis (lead); Investigation (equal); Writing – original draft (lead); Writing – review & editing (equal). **Joel Daou:** Conceptualization (equal); Formal analysis (supporting); Funding acquisition (lead); Investigation (equal); Writing – original draft (lead); Writing – review & editing (equal).

## DATA AVAILABILITY

The data that support the findings of this study are available within the article.

## REFERENCES

[1]E. Al Sarraf, C. Almarcha, J. Quinard, B. Radisson, B. Denet, and P. Garcia-Ybarra, "Darrieus–Landau instability and Markstein numbers of premixed flames in a Hele-Shaw cell," Proc. Combust. Inst. **37**, 1783–1789 (2019).
[2]A. Dejoan, Z. Zhou, D. Fernández-Galisteo, P. D. Ronney, and V. N. Kurdyumov, "Effect of confinement on the propagation patterns of lean hydrogen–air flames," Proc. Combust. Inst. **40**, 105431 (2024).
[3]D. Fernández-Galisteo, V. N. Kurdyumov, and P. D. Ronney, "Analysis of premixed flame propagation between two closely-spaced parallel plates," Combust. Flame **190**, 133–145 (2018).
[4]F. Veiga-López, D. Martínez-Ruiz, E. Fernández-Tarrazo, and M. Sánchez-Sanz, "Experimental analysis of oscillatory premixed flames in a Hele-Shaw cell propagating towards a closed end," Combust. Flame **201**, 1–11 (2019).
[5]F. Veiga-López, M. Kuznetsov, D. Martínez-Ruiz, E. Fernández-Tarrazo, J. Grune, and M. Sánchez-Sanz, "Unexpected propagation of ultra-lean hydrogen flames in narrow gaps," Phys. Rev. Lett. **124**, 174501 (2020).
[6]D. Martínez-Ruiz, F. Veiga-López, D. Fernández-Galisteo, V. N. Kurdyumov, and M. Sánchez-Sanz, "The role of conductive heat losses on the formation of isolated flame cells in Hele-Shaw chambers," Combust. Flame **209**, 187–199 (2019).
[7]P. Rajamanickam and J. Daou, "Effect of a shear flow on the Darrieus–Landau instability in a Hele-Shaw channel," Proc. Combust. Inst. **40**, 105671 (2024).
[8]D. Fernández-Galisteo and V. N. Kurdyumov, "Impact of the gravity field on stability of premixed flames propagating between two closely spaced parallel plates," Proc. Combust. Inst. **37**, 1937–1943 (2019).
[9]J. Daou and P. Rajamanickam, "Hydrodynamic instabilities of propagating interfaces under Darcy's law," Phys. Rev. Fluids (to be published) (2024).
[10]G. Joulin and G. I. Sivashinsky, "Influence of momentum and heat losses on the large-scale stability of quasi-2d premixed flames," Combust. Sci. Technol. **98**, 11–23 (1994).
[11]T. Miroshnichenko, V. Gubernov, and S. Minaev, "Hydrodynamic instability of premixed flame propagating in narrow planar channel in the presence of gas flow," Combust. Theory Model. **24**, 362–375 (2020).
[12]G. I. Sivashinsky, "Nonlinear analysis of hydrodynamic instability in laminar flames–i. derivation of basic equations," in *Dynamics of Curved Fronts* (Elsevier, 1977), pp. 459–488.
[13]P. Clavin and F. A. Williams, "Effects of molecular diffusion and of thermal expansion on the structure and dynamics of premixed flames in turbulent flows of large scale and low intensity," J. Fluid Mech. **116**, 251–282 (1982).
[14]P. Pelce and P. Clavin, "Influence of hydrodynamics and diffusion upon the stability limits of laminar premixed flames," in *Dynamics of Curved Fronts* (Elsevier, 1988) pp. 425–443.

[15]M. Matalon and B. J. Matkowsky, "Flames as gasdynamic discontinuities," J. Fluid Mech. **124**, 239–259 (1982).
[16]P. Clavin and G. Joulin, "Premixed flames in large scale and high intensity turbulent flow," J. Phyique. Lett. **44**, 1–12 (1983).
[17]P. Clavin and P. Garcia, "The influence of the temperature dependence of diffusivities on the dynamics," J. de Méc. Théorique Appl. **2**, 245–263 (1983).
[18]P. Garcia-Ybarra, C. Nicoli, and P. Clavin, "Soret and dilution effects on premixed flames," Combust. Sci. Technol. **42**, 87–109 (1984).
[19]P. Clavin and C. Nicoli, "Effect of heat losses on the limits of stability of premixed flames propagating downwards," Combust. Flame **60**, 1–14 (1985).
[20]D. Keller and N. Peters, "Transient pressure effects in the evolution equation for premixed flame fronts," Theoret. Comput. Fluid Dyn. **6–6**, 141–159 (1994).
[21]M. Matalon, C. Cui, and J. K. Bechtold, "Hydrodynamic theory of premixed flames: Effects of stoichiometry, variable transport coefficients and arbitrary reaction orders," J. Fluid Mech. **487**, 179–210 (2003).
[22]M. Matalon and J. K. Bechtold, "A multi-scale approach to the propagation of non-adiabatic premixed flames," J. Eng. Math. **63**, 309–326 (2009).
[23]P. Clavin and J. C. Graña-Otero, "Curved and stretched flames: The two markstein numbers," J. Fluid Mech. **686**, 187–217 (2011).
[24]J. K. Bechtold, G. Krishnan, and M. Matalon, "Hydrodynamic theory of premixed flames propagating in closed vessels: Flame speed and Markstein lengths," J. Fluid Mech. **998**, A59 (2024).
[25]F. A. Williams, "Turbulent combustion," in *The Mathematics of Combustion* (SIAM, 1985), pp. 97–131.
[26]J. K. Bechtold and M. Matalon, "The dependence of the Markstein length on stoichiometry," Combust. Flame **127**, 1906–1913 (2001).
[27]The analysis of Keller and Peters[20] differs from others in the sense that the former works in a fixed Cartesian coordinate system $(\mathbf{x}, t)$ instead of the flame-fixed coordinate system.
[28]P. Clavin and G. Searby, *Combustion Waves and Fronts in Flows: Flames, Shocks, Detonations, Ablation Fronts and Explosion of Stars* (Cambridge University Press, 2016).
[29]Specifically, using the leading-order outer $G$-equation $\bar{\rho}\tilde{D}G/\tilde{D}t = |\nabla G|$ given in (17), we find following Keller and Peters [20] that $\tilde{D}|\nabla G|/\tilde{D}t = (1/\bar{\rho})\mathbf{n}\cdot\nabla|\nabla G| - \mathbf{nn}:\nabla\mathbf{V}_0|\nabla G|$ and $\nabla^2 G = \mathbf{n}\cdot\nabla|\nabla G| + |\nabla G|\nabla\cdot\mathbf{n}$, which simplifies the first two terms on the right side of (23). To simplify the last term, we note that for an arbitrary vector $\mathbf{A}$, $\mathcal{P}\mathbf{A} = \mathbf{n}\times(\mathbf{A}\times\mathbf{n})$ and hence $\nabla\cdot[|\nabla G|\mathcal{P}\mathbf{A}] = -\nabla G\cdot[\nabla\times(\mathbf{A}\times\mathbf{n})]$; dividing by $|\nabla G|$, we thus obtain $\nabla\cdot[|\nabla G|\mathcal{P}\mathbf{A}]/|\nabla G| = -\mathbf{n}\cdot\nabla\times(\mathbf{A}\times\mathbf{n}) = -(\mathbf{A}\cdot\mathbf{n})(\nabla\cdot\mathbf{n}) - \mathbf{nn}:\nabla\mathbf{A}$, upon imposing the condition $\nabla\cdot\mathbf{A} = 0$.
[30]The simplifications use the relation $\lambda_0\partial\theta_0/\partial\zeta = \theta_0/|\nabla G|$ and the fact that $\nabla\theta_0 = 0$ at $\zeta = 0$ which follow from the expression of $\theta_0$ in (13).
[31]G. K. Giannakopoulos, A. Gatzoulis, C. E. Frouzakis, M. Matalon, and A. G. Tomboulides, "Consistent definitions of "flame displacement speed" and "Markstein length" for premixed flame propagation," Combust. Flame **162**, 1249–1264 (2015).
[32]G. K. Giannakopoulos, C. E. Frouzakis, S. Mohan, A. G. Tomboulides, and M. Matalon, "Consumption and displacement speeds of stretched premixed flames-theory and simulations," Combust. Flame **208**, 164–181 (2019).